Thermal behavior in rolling bearing applications: Comparison of steel and ceramic materials applied to tapered rollers

Charlotte Fossier, Thomas Touret, Guillaume Lefort, Christophe Changenet

Thermal behavior in rolling bearing applications: comparison of steel and ceramic materials applied to tapered rollers

By:
Charlotte Fossier[1) *]
Thomas Touret[2)],
Guillaume Lefort[1)]
Christophe Changenet[2)]

[1)]NTN in Europe, France
[2)]Univ. Lyon, ECAM LaSalle, LabECAM, France.

To cite this article please refer to the journal version of the article at:
DOI : https://doi.org/10.1177/13506501221144357

Thermal behavior in rolling bearing applications: comparison of steel and ceramic materials applied to tapered rollers

Charlotte Fossier[1) *], Thomas Touret[2)], Guillaume Lefort[1)], and Christophe Changenet[2)]

[1)]NTN in Europe, France
[2)]Univ. Lyon, ECAM LaSalle, LabECAM, France.
*Corresponding author: charlotte.fossier@ntn-snr.fr

Due to their properties, ceramic materials can improve both reliability and efficiency of rolling bearings. Most of the studies have investigated the power losses and temperatures of ball bearings with balls made of silicon nitride (Si_3N_4) versus steel ones. This study thus focuses on tapered rollers. Thanks to experimental and numerical means, the thermal behavior of tapered roller bearing is investigated for both steel and silicon nitride rollers. Various operating conditions (rotational speed, oil flow rate and oil temperature) are tested to allow the comparison of the behavior of both bearing set-ups (full-steel and hybrid). A thermal model is developed according to the thermal network method and is validated thanks to experimental results. It is then used to analyze behaviors observed during experiments, related to thermal exchanges and power losses. The effect of changing the mechanical and thermal properties of the roller material is investigated.

Keywords: rolling element bearing, tapered roller bearing, ceramic, silicon nitride, hybrid bearing, thermal behavior, heat flow

1. Introduction

The use of ceramic material, and more specifically of silicon nitride (Si_3N_4), in bearings offers new possibilities in terms of performance. The aeronautic industry is particularly interested by the development of this technology with two focuses: reliability and efficiency. Indeed, several improvements could be expected:

1) Silicon nitride has a lower density than steel; the weight gain is interesting for efficiency perspectives; regarding ceramic rolling elements, it could also decrease centrifugal forces and so bearing stress.

2) Silicon nitride has a better reliability than steel regarding contamination and lubrication starvation [1] which can lead to an improvement in bearing rating life.

3) Silicon nitride balls appear to dissipate less power than steel ones [2]; so, bearing efficiency can be improved; it could also induce a lower lubricant temperature and so improve bearing operating conditions.

As it has been above-mentioned, one of the main advantages of hybrid ball bearings is the reduction of centrifugal forces [3,4], due to the low density of silicon nitride balls; thus, the load on outer ring contacts is reduced. This is particularly important when rotational speeds lead to the range of 1 to 3 million $D.N$ (bore diameter (mm) $\times$ shaft rotational speed (rpm)), which corresponds to the high-speed domain. A gain on bearing efficiency is thus expected with hybrid ball bearings: Cento and Dareing [3] estimated by computations that a hybrid radial ball bearing dissipates 20% less than a full-steel one; Paleu et al. [4] calculated that the power loss of an angular contact ball bearing is decreased by 30 to 50% for normal- and high-speed ranges thanks to the use of ceramic balls; Gloekner et al. [2] measured that a hybrid ball bearing has lower power losses than a full-steel one for the speed range 2.5 to 2.8 million $D.N$ (5 to 8% less).

Some of these authors also covered the normal speed range (below 1 million $D.N$) and noticed a slight reduction of power losses thanks to hybrid ball bearings, ranging from 5% [3] to 30% [4]. However, as they focused on high-speed results, they did not investigate the reason for power loss reduction in the normal speed range. Indeed, hybrid bearings were mainly studied for high-speed applications such as machine tool spindles or aircraft engines; studies at normal speeds are thus lacking.

The use of ceramic rolling elements could also affect the thermal behavior of the bearing. Shoda et al. [5] showed experimentally that at high speed a rolling element bearing with silicon nitride balls operates with a lower temperature difference between inner ring and outer ring when compared to a full-steel one; the authors related this directly to the power losses and so to the heat generation inside each contact. Indeed, due to centrifugal forces, a greater load is applied on outer ring contacts of full-steel bearing, leading to a greater heat generation and temperature elevation. Also due to this difference on centrifugal forces, Gloekner et al. [2] measured a higher outer ring temperature for a full-steel ball bearing than for a hybrid one. Paleu et al. [6] measured the equilibrium temperature of full-steel, hybrid and partial hybrid (mix of steel and ceramic rolling elements) angular contact ball bearings. They observed that the full-steel bearing has the greater operating temperature and the hybrid bearing has the lowest one, the partial hybrid bearing being in-between; they explained this by the reduced centrifugal forces of hybrid bearing and so by lower power losses; they also suggested that the smaller contact area obtained with silicon nitride balls may be an additional reason, without specifying if this was related to contact friction or thermal exchanges. Aramaki et al. [7] studied angular contact ball bearings under poor lubrication (oil-air lubrication or small amount of grease) by measuring the outer ring steady-state temperature; they observed a more regular increase of the hybrid bearing operating temperature with speed, while for a full-steel one the increase is greater at normal speed and even sharper at high speed. Influence of materials on contact temperature was also highlighted in a recent study based on *In Situ* measurements [X].

Most of those studies stated that the same internal geometry is used for both full-steel and hybrid ball bearings (i.e. same race conformity [3,4]) and that the only change is the rolling elements themselves. For the same applied load (and without considering centrifugal forces), a greater contact pressure is thus expected in the hybrid bearings due to the ball

material stiffness.

All those studies were conducted on ball bearings. However, in the case of hybrid tapered roller bearings operating at lower speed range (up to 0.5 million $D.N$ in the present study; up to 1 million $D.N$ in applications), centrifugal forces are less important and the power loss difference between bearings with steel and silicon nitride rollers might be limited. This paper thus aims at investigating the effect of the use of silicon nitride tapered rollers compared to steel ones for an aeronautic application regarding power losses and bearing temperature distribution. Temperature measurements will give a first comparison. A numerical model will then allow to study both power losses and heat flows and their consequences on the temperature distribution inside the bearing.

2. Testing campaign

2.1. Tested bearings

Two set-ups of tapered roller bearings (TRB) are tested: a full-steel and a hybrid one where the rollers are made out of ceramic. Their dimensions and geometries are identical; some details are given in Table 1. A similar surface roughness ($0.06 \leq Ra \leq 0.10$ µm) is achieved on steel and ceramic rollers and their geometry is exactly the same. For both bearing set-ups, the rings are made of M50 steel. The full-steel bearings have M50 steel rollers and the hybrid bearings have silicon nitride (Si_3N_4) rollers. These bearings are lubricated with a MIL-PRF-23699 oil, whose properties are given in Table 2.

Table 1: Geometry of the tapered roller bearing

Parameter	**Value**
Outer diameter [mm]	130
Inner diameter [mm]	75
Width [mm]	33
Cup angle [°]	16
Roller length [mm]	18.8
Roller max. diameter [mm]	15.6
Number of rollers	9

Table 2: Properties of the oil

Parameter	**Value**
Kinematic viscosity at 40°C [cSt]	27.6
Kinematic viscosity at 100°C [cSt]	5.1
Density at 15°C [kg/m^3]	1003
Thermal conductivity [W/m.K]	0.152
Specific heat [J/kg.K]	2000

2.2. Test rig

The standard bearing rig illustrated on

Figure 1 is used; two TRBs with the same set-up (full-steel or hybrid) are tested at a time. This rig allows varying shaft rotational speed, input oil temperature and oil flow rate. Oil is injected on both sides of the tested tapered roller bearings. An axial load F_a is always applied to the tested bearings and an additional radial load F_r can be applied thanks to two cylindrical roller bearings that are glide fitted to avoid impact on the axial loading. The loads (axial and radial) are transmitted to the bearing assembly by springs. They are controlled by a calibrated load cell at the beginning of each test condition. Component temperatures, such as inner and outer rings of bearings, oil inlet and outlet, are monitored. The two sensors on each TRB outer ring are located in the radially unloaded zone (upper zone), due to bench architecture constraint.

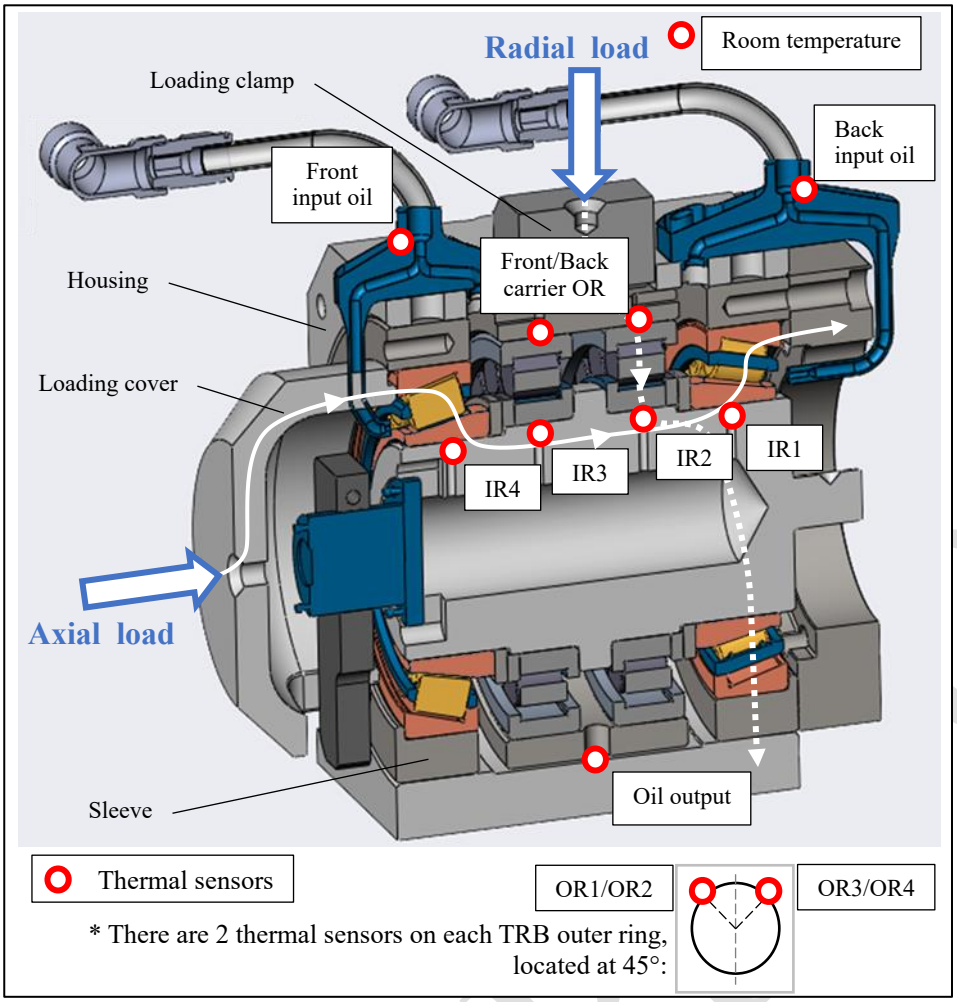

Figure 1: Test assembly with thermal sensor locations

2.3. Test plan

Parametric tests are performed on both set-ups of tapered roller bearing (with steel or ceramic rollers). Several operating parameters are varied: shaft rotational speed, input oil temperature, and oil flow rate. The same load is applied for both set-ups, as the aim is to replace the full-steel bearing by a hybrid bearing on an application. It results in different contact pressures as material stiffness is different. The complete list of these tests is given in Table 3 for both bearing set-ups.

Table 3: Conditions of the parametric tests

Condition	Value
Test bearing applied load and contact pressure	F_a = 20 000 N / F_r = 15 000 N Contact pressure = 2.34 GPa for the full-steel bearing = 2.60 GPa for the hybrid bearing
Oil inlet temperature	40°C, 70°C
Oil flow rate	1.5L/min, 2.3 L/min
Rotational Speed	2250 rpm, 4500 rpm

2.4. Test results

Temperatures measured during the steady-state operation are now analyzed; this stabilized regime is reached after roughly 1 hour of operation; the measurement results presented are a mean over 5 minutes. Experimental results are presented hereafter through a comparison of measurements done on full-steel bearings and hybrid bearings during steady-state operation. An average temperature of the bearing T_{av} is defined as the average between inner ring and outer ring temperatures in stabilized regime. As temperature difference between the two TRBs is limited, only the front bearing is considered. Then $\Delta T_{hybrid-fullsteel}$, which corresponds to the difference on T_{av} between bearings with ceramic rollers and with steel rollers, is determined as:

$$\Delta T_{hybrid-fullsteel} = T_{av\ hybrid} - T_{av\ fullsteel}$$

Figure 2 presents $\Delta T_{hybrid-fullsteel}$ for every test condition. The average bearing temperature is always higher with the hybrid bearing (from 2.7°C to 12°C higher compared to the full-steel bearing). This difference on average temperature

is aggravated by the increase of the rotational speed.
Figure 3 presents the difference between inner ring (IR) and outer ring (OR) temperatures for both bearing types. The outer ring temperature corresponds to the average temperature of the two OR temperatures that are measured on a same TRB (refer to
Figure 1 for sensor locations). The temperature difference between IR and OR tends to be greater with hybrid bearing whatever the condition (up to +5°C greater compared to full-steel bearing). Moreover, it appears that a lower injection temperature induces a greater difference on the temperature distribution between a full-steel and a hybrid TRB.

These two experimental observations made on tapered roller bearings are different from the ones obtained by previous studies with hybrid ball bearings. Indeed, both bearing average temperature [6] and temperature difference between IR and OR [5] were lower for hybrid ball bearing, while here they are greater for tapered roller bearing.

The increase of both average temperatures and ring temperature differences of the hybrid bearing may be attributed to an increase of the power losses, especially as it is strongly correlated to the rotational speed. Yet the conduction phenomenon due to the change of roller materials can also have an impact on this observation and must be studied.

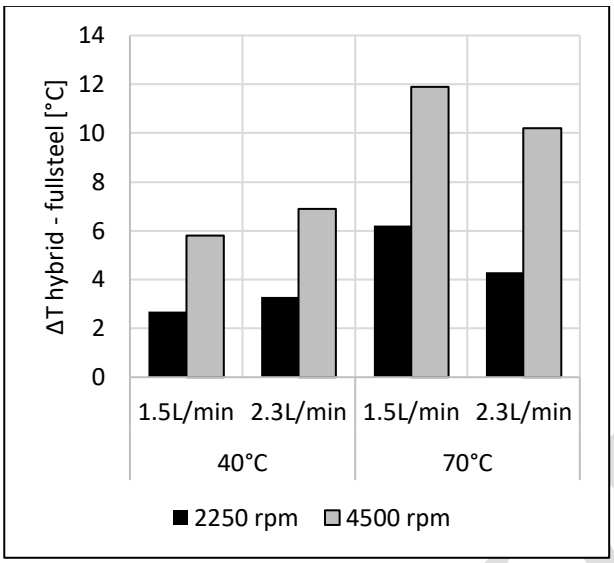

Figure 2: $\Delta T_{hybrid-fullsteel}$ for steady state experimental results (a positive value indicates that hybrid T_{av} is higher than full-steel T_{av})

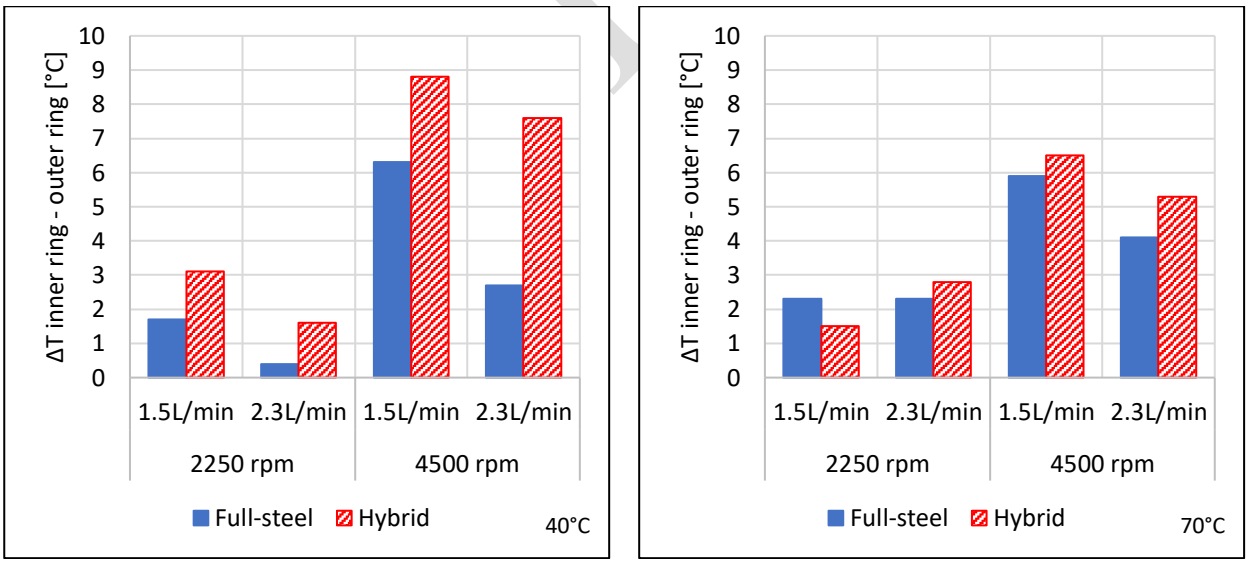

Figure 3: Difference of temperature between inner and outer rings for both full-steel and hybrid bearings for steady state experimental results with oil inlet temperature at 40°C (left) and 70°C (right) (a positive value indicates that IR temperature is higher than OR temperature)

3. Changing the roller material

The difference between both bearing set-ups is the material of the rollers: ceramic (Si_3N_4) instead of steel. This induces a modification of material properties: mechanical properties, such as the elastic modulus, the Poisson's coefficient and the density, and thermal properties, such as the thermal conductivity and the specific heat. The values of these mechanical and thermal properties are given in Table 4. The change of material properties has several effects that could explain the

experimental observations made previously; these effects are discussed hereafter.

Table 4: Material properties of steel and ceramic

	Elastic modulus [GPa]	**Poisson's coefficient [-]**	**Density [kg/m^3]**	**Thermal conductivity [W/m.K]**	**Specific heat [J/kg.K]**
Steel (M50)	202	0.29	7 800	50	470
Ceramic (Si_3N_4)	300	0.26	3 250	30	800

3.1. Mechanical properties – Size of contact area

The modification of elastic modulus and Poisson's coefficient impacts directly the size of contacts: for the same applied load, contacts will be smaller in the case of ceramic rollers. As an example, the size of roller–raceway contact area in test conditions of Table 3 is smaller for hybrid bearings: on average, the contact area is reduced by 7% according to calculations.

This difference of contact size could have a direct effect on power losses for ceramic rollers, due to two phenomena:

- increase of the contact pressure compared to steel rollers, due to the application of the same load on a smaller area; this tends to increase power losses.
- decrease of the contact area where friction occurs; this tends to decrease power losses.

The size of the contact has also an impact on thermal exchanges between rollers and rings; they will be reduced for ceramic rollers due to the smaller exchange area.

3.2. Thermal properties

The modification of the thermal properties of rollers impacts the heat transfer between rollers and raceways. This may change the temperature distribution of the tapered roller bearing.

3.3. Contact friction

Apart from the material properties already described, the use of ceramic rollers may also modify the contact friction from a tribological perspective. In the case of boundary and mixed lubrication regimes, the friction coefficient depends on the interactions between surface asperities. The change of surface material could influence the friction coefficient due to the asperity interactions thanks to several effects:

- Friction of a steel surface and a ceramic surface (instead of two steel surfaces);
- Possible reaction of lubricant with ceramic surface in addition to possible reaction with steel surface; a tribo-film could be created, that modifies the friction of surfaces.

These modifications can directly impact the power losses of the hybrid bearing compared to the steel one.

4. Thermal model of the test rig

Both power losses and material properties could have an impact on the thermal behavior difference that is observed between steel and hybrid bearings. In order to better understand these experimental findings presented in Part 2.4. , a thermal model of the set-up was established with the aim of studying separately the influence of power losses and thermal properties of rollers.

4.1. Thermal network method

The thermal network approach employed in this study is a nodal model. It can compute the bulk temperatures of a given system considering that each component of the modelled system is an isothermal node [8]. Heat flux between the nodes are modelled thanks to thermal resistances considering simplified geometry and using classical heat transfer equations. The heat produced by power losses is injected on the corresponding node.

Temperatures are then estimated by solving the first principle of thermodynamics on each node (i) of the network:

$$M_i c_i \frac{dT_i}{dt} = Q_i + \sum_{j=1\ \&\ j\neq 1}^{n} \frac{T_j - T_i}{R_{Th}(i,j)}$$

With:

M_i : Mass [kg]

c_i : Thermal capacity [J / kg °K]

T_i : Temperature [°C]

Q_i : Heat flux [W]

$R_{Th}(i,j)$: Thermal resistance [K/W]

Temperature and heat flux distributions can be estimated by solving the thermal network as explained in [8].

4.2. Thermal network of the test rig

Due to symmetry, only half of the test rig is modelled. The test rig is decomposed in isothermal nodes according to the thermal network methodology [8]. The complete node list is given in Table 5; it should be noticed that the outer ring of the tested bearing is separated in two parts: the lower part encompasses the loaded zone and the upper part is the unloaded zone. The tested tapered roller bearing is discretized precisely as proposed by Pouly et al. [9] to determine accurately its temperature distribution. The carrier bearing is simply modeled with 4 nodes according to Niel et al. [10], as it is of lower interest.

Nodes and thermal resistances interconnection results in a network that can be represented as in Figure 4. The nodes related to ambient air (1), oil injection (2) and foundation (3) are boundary conditions of the model and their temperature is imposed.

Table 5: Node description

Node	Full designation in the model
1	Ambient air
2	Injection
3	Foundation
4	Bench
5	Bearing oil
6	Deflected oil
7	Upper housing
8	Lower housing
9	Upper sleeve
10	Lower sleeve
11	Loading cover
12	Shaft
13	TRB upper Outer Ring
14	TRB lower Outer Ring
15	TRB inner ring
16	TRB cage
17	TRB rollers
18	Striction zone between rollers and upper outer ring
19	Striction zone between rollers and lower outer ring
20	Striction zone between rollers and inner ring
21	Loading clamp
22	Carrier housing
23	Carrier Outer Ring
24	Carrier Rolling Elements
25	Carrier Inner Ring
26	Carrier oil

4.3. Power loss sources

To simulate heat generation in the model, power losses are injected to specific nodes of the thermal network. In this study, power losses are estimated thanks to SharcNT engineering software developed by NTN [11]. This includes power losses at contacts (sliding friction at roller-race and roller-rib contacts; rolling resistance at roller-race contacts) and those due to drag. The sliding friction in the roller-race contacts is estimated thanks to the theory of Greenwood and Tripp [Z] to allow the combination of fluid friction and asperities friction, and thus consider the various lubrication regimes (full film, mixed and boundary); a rheological model based on Ree-Eyring [Y] is used to compute the fluid shear stress. For the roller-rib contact, the sliding friction is calculated according to the work of Aihara on tapered roller bearings [ref to be added].

The power losses are estimated with SharcNT for all tested operating conditions: load, speed and flow rate as given in Table 3, and lubricant properties as given in Table 2. These calculations are performed for various temperatures, ranging from 20°C to 160°C, with increment of 20°C. The Solver of the thermal network then interpolates power losses according to the temperature of the considered node. This allows to compute the thermal coupling as described in [8].

Contact losses are injected in their respective striction nodes (18, 19, 20). Drag losses are added to the oil node that is associated with the bearing (5). Conversely, the temperature of each striction node (18, 19, 20) is considered for the power loss estimation of the respective contact, and the temperature of the bearing oil node (5) is considered for the estimation of drag loss.

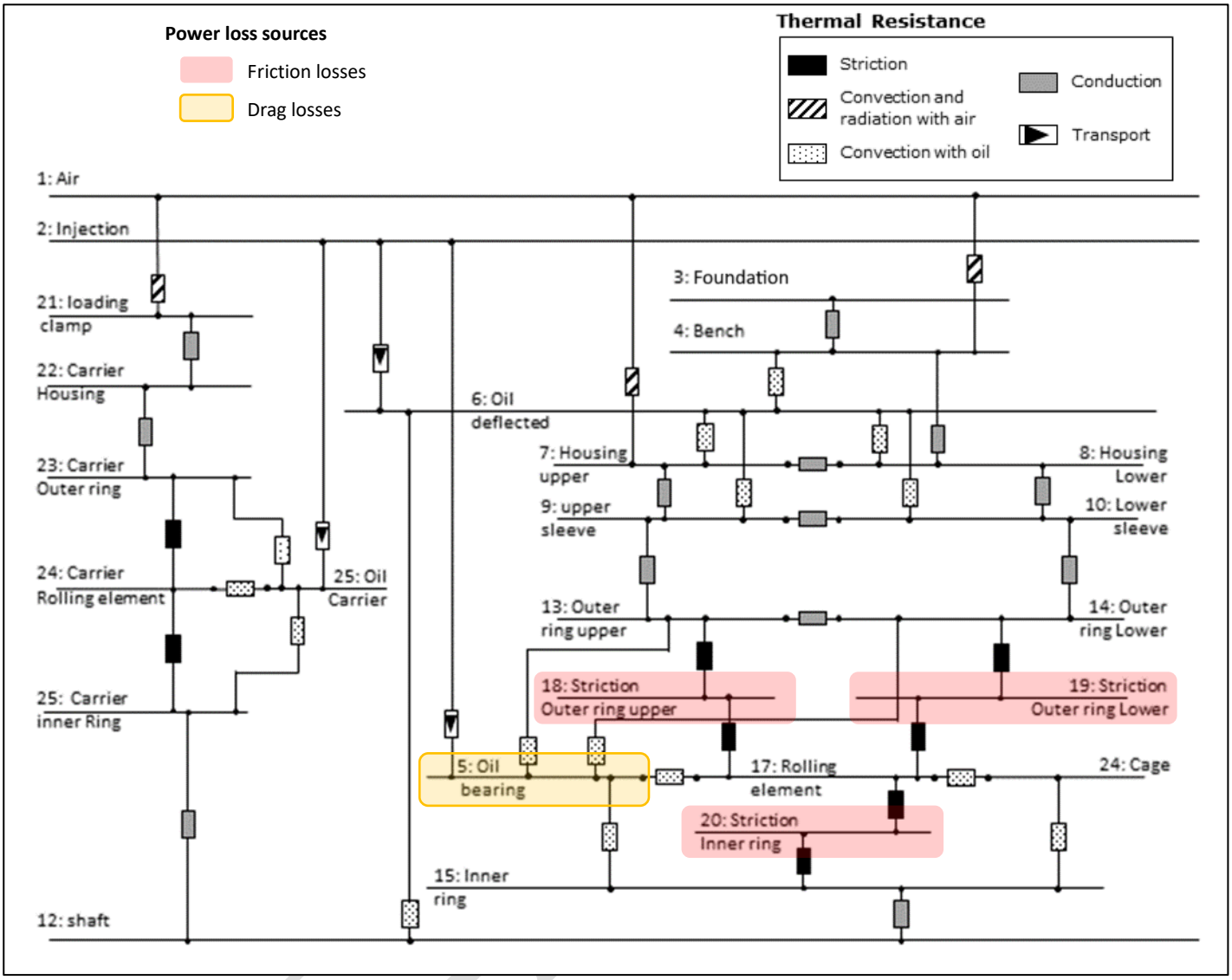

Figure 4: The thermal network of the test rig

4.4. Thermal resistances

To determine the heat exchanges that occur inside the thermal network of the test rig, the following thermal resistances are used:

1. Thermal resistances of convection and radiation between the bench and the surrounding air are respectively estimated thanks to Newton's and Stephan-Boltzmann's laws [12]; the bench housing is considered as an assembly of plates, so that classic correlations for flat plates are used to determine air convection;
2. Thermal resistances of conduction between components are estimated thanks to Fourier's law [12], as these exchanges occurs on cylindrical parts;
3. Thermal resistances of transport are estimated as explained by Pouly et al. [9]; this simulates the heat absorption by the oil, depending on oil flow rate and oil heat capacity;
4. Thermal resistances of convection with oil are estimated according to various formulae [13], to consider oil forced convection with components and oil flow along vertical surfaces.
5. Thermal resistances of striction allow to simulate the heat flux at the contact between two moving components, as this flux is confined within the contact area. This conduction phenomenon can be modelled from Blok formulation as proposed by Changenet [8,14]:

$$R_{striction} = \left(\sum_{j}^{Z} \left(\frac{0.918}{2 \cdot b_j \cdot \chi \cdot \sqrt{2 \cdot a_j \cdot V_R}} \right)^{-1} \right)^{-1}$$

With:

Z: number of balls

b_j : Elliptical contact width for ball j [m]

a_j : Elliptical contact length for ball j [m]

V_R : Contact velocity [m/s]

χ : Material effusivity [N/ms$^{1/2}$K], $\chi = \sqrt{k\,\rho\,c}$ with k the material thermal conductivity [W/m.K], ρ the material density [kg/m^3], and c the material specific heat [J/kg.K]

When the material of the roller is changed from steel to ceramic, the thermal resistances of striction between rollers and raceways are impacted in two ways: modification of thermal properties of the material (material effusivity χ) and modification of mechanical properties of the material (that changes the size of contact area). The thermal model uses the contact size calculated by SharcNT tool.

5. Model validation with full-steel bearings

The results given by the thermal network model of the test rig are compared to experimental measurements.

The first step is to validate heat transfers between the test bench and its environment. Therefore, a calibration test was performed by recording the cooling of the bench after operation: the bench is stopped (no more rotation, no more oil flow); the temperature of components is measured until the temperature of tested bearings reaches the ambient air temperature (roughly 3 to 4 hours). Figure 5 shows the results of the cooling test and simulation. The measured temperatures of IR and OR decrease with time, as the bench cools down; IR and OR measured temperatures are slightly different from each other at the beginning due to previous test conditions. IR and OR calculated temperatures are identical because they numerically start at the same temperature; moreover, they have similar heat exchanges. The good correlation validates the formulations proposed to model heat exchanges by conduction and convection with air.

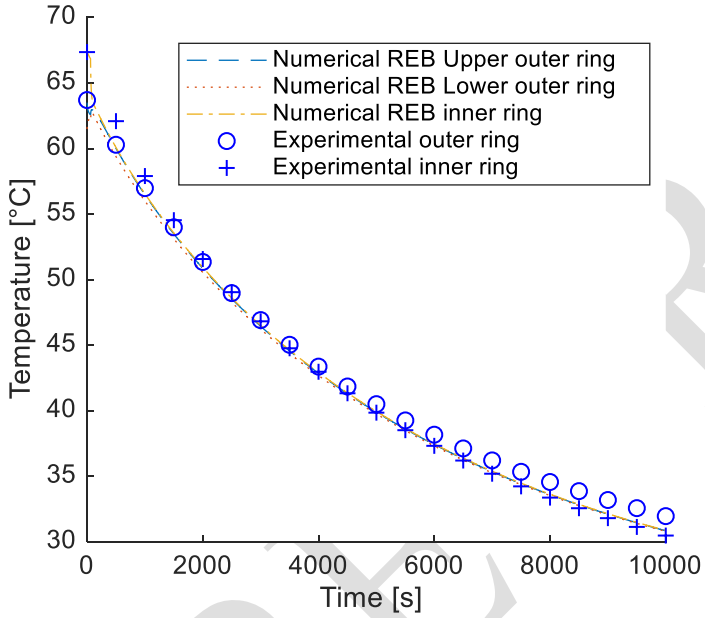

Figure 5 : Comparison between numerical and experimental temperature results for the cooling test

On Figure 6, the model results are now compared to the measurements obtained with full-steel bearings during the parametric tests with an injection temperature of 70°C. This will assess the validity of both power losses and convection heat exchange with oil. Each graph corresponds to different conditions of rotational speed and lubrication (flow rate and temperature). It should be noticed that the numerical upper OR temperature should correspond to the measured OR temperature, as the OR temperature sensors are located on the upper part of the bearings.

The bearing temperature variation in dynamic regime is well modeled in these comparisons: calculation results follow the same trends as measurements. The bearing average temperature in stabilized regime is also accurately modelled in all regimes, as recapitulated in Table 6. Indeed, temperature difference between experiments and calculations is in the range of +/-2°C. A good correlation is thus obtained with the model of the full-steel bearing.

Figure 7 presents a comparison between measurements and calculations of the temperature elevation of IR and OR (relatively to oil inlet temperature) of the full-steel bearing in stabilized regime. The estimated power losses are also given. Measured and calculated temperature elevation follow the same trend: for each lubrication condition, it increases with rotational speed; so are the estimated power losses. The different contribution of the generated heat change with operating condition, nevertheless, contacts between rollers and inner ring are the main source of dissipation. When lubrication temperature is higher (70°C), the temperature elevation of the rings is lower, as power losses are reduced by a lower oil viscosity.

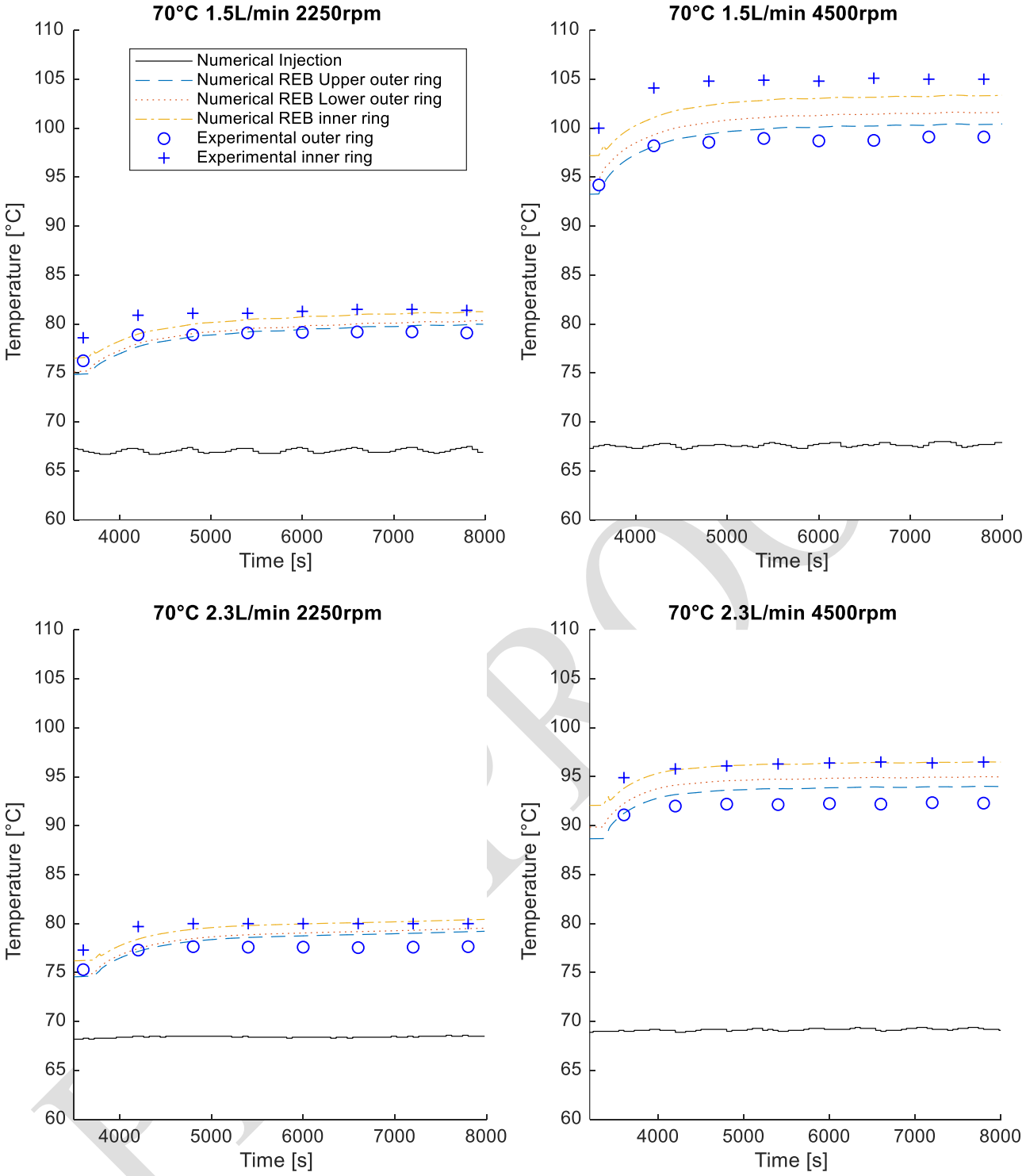

Figure 6 : Correlation between simulation and experiment for full steel bearing (injection temperature of 70°C)

Table 6: Temperature difference between simulated and experimental bearing average temperatures in stabilized regime with steel tapered rollers (a positive value indicates that simulated temperature is higher than measured temperature)

Oil temperature (°C)	**40**				**70**			
Oil flow (L/min)	**1.5**		**2.3**		**1.5**		**2.3**	
Rotation speed (rpm)	**2250**	**4500**	**2250**	**4500**	**2250**	**4500**	**2250**	**4500**
Temperature difference (°C)	-0.9	+1.0	+2.2	+1.6	+0.2	-0.1	+0.9	+0.8

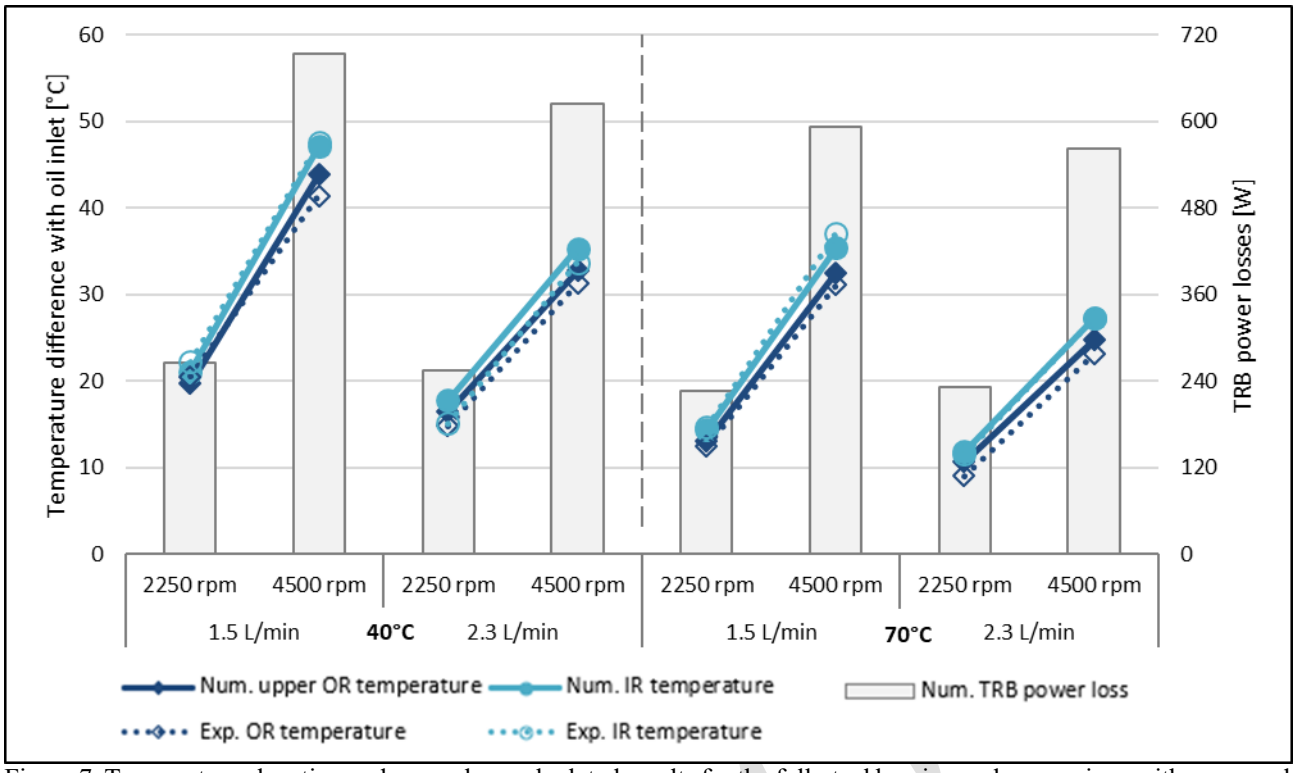

Figure 7: Temperature elevation and power loss calculated results for the full-steel bearing and comparison with measured temperature elevation in stabilized regime

6. Numerical comparison with hybrid bearings

The same thermal network model is used for the hybrid bearing. As hybrid bearings are completely identical to full-steel bearings from a geometric point of view, all convective heat transfers with oil are considered identical. Other thermal exchanges between the bearing rings and the bench or between the bench and its environment are also identical.

According to SharcNT results, the lubrication regime for the most loaded IR contact and the rib contact is mixed ($1 < \lambda < 3$, where λ is the ratio between contact film thickness and surface roughness) for every operating condition and both bearing set-ups, when considering the experimental IR temperature (most loaded roller–raceway contact) and OR temperatures (rib–roller end contact). Therefore, asperity interactions may have a slight impact on contact friction. In a first approach, the comparison between full-steel and hybrid bearings is done by using the same friction law. For the same operating conditions, the hybrid bearing has greater contact pressures but smaller contacts. In the studied case, this results in lower calculated power losses.

Figure 8 presents the measured and calculated temperature elevations of IR and OR (relatively to oil inlet temperature) and the power losses for the hybrid bearing in stabilized regime. As for full-steel bearings, measured and calculated temperature elevation and estimated power losses follow the same trend: for each lubrication condition, it increases with rotational speed; when the lubricant temperature is greater (70°C), the bearing temperature elevation is lower and power losses are reduced, due to a lower oil viscosity. However, contrary to the results with full-steel bearing that correlate well, it appears that the estimated temperature elevation of hybrid bearing is lower than the measured one, for both IR and OR, and thus also for bearing average temperature.

Thermal exchanges between the bearing and the oil or between the bearing and the bench are identical for both full-steel and hybrid bearings. Thus, the difference can be explained in two ways. The first one is the thermal exchanges between rollers and raceways that are modified by the change of roller material and might induce the increase of bearing average temperature observed experimentally. The second one is that power losses of the hybrid bearing are underestimated. This is supported by the fact that the discrepancy on temperature elevation tends to be greater with higher speed (more power losses) and with lower oil flow rate (less heat dissipation). Following section will investigate these assumptions based on simulations conducted with the thermal network.

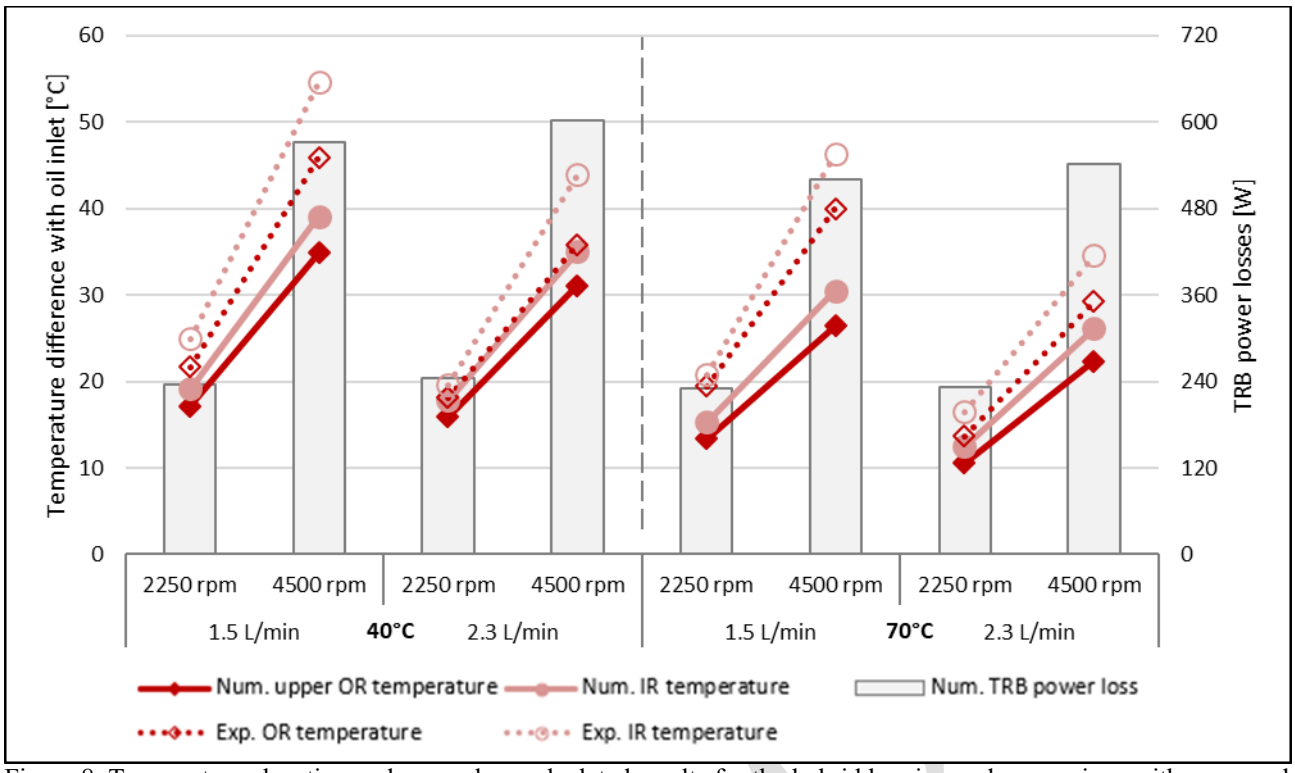

Figure 8: Temperature elevation and power loss calculated results for the hybrid bearing and comparison with measured temperature elevation in stabilized regime

7. Discussion

Experimental results presented in Part 2.4. highlighted that the average bearing temperature is higher with hybrid tapered roller bearing than with full-steel bearing. Moreover, a greater temperature difference exists between IR and OR for hybrid tapered roller bearing than for full-steel bearing. The thermal network is used here to investigate if these differences are induced by material properties, as this model allows to study the impact of material properties independently from power losses.

7.1. Impact of both mechanical and thermal material properties

The same power losses are then inputted, whatever the material of rolling elements (steel or ceramic). The same temperatures of boundary conditions and injection rate are also used (from the steel bearing experiments). Mechanical and thermal material properties are changed depending on the material simulated, according to Table 4. As a result, contact surface area and roller thermal properties are modified in the simulation, changing the thermal exchanges between rollers and raceways.

The corresponding simulation is presented in Figure 9 for two operating conditions. The temperature of IR and OR is presented for both roller materials. It appears that changing mechanical and thermal material properties from steel to ceramic increases the temperature difference between the inner ring and the outer ring. This increase in temperature difference ranges from 1 to 3°C depending on operating conditions (+55% on temperature difference between IR and OR). This is consistent with the experimental results where this difference is 1.5°C on average and is up to 4°C.

Yet changing mechanical and thermal material properties do not change the average temperature of the bearing. This simulation tends to validate the fact that power losses are increased when switching roller material as presented in the previous section.

7.2. Impact of thermal material properties alone

To go further on thermal exchanges, another simulation is performed by changing only the thermal properties of the rolling elements. Mechanical properties of the material are kept the same, so contact surfaces in the bearing are the one calculated with steel rollers.

The temperature difference between IR and OR is increased by 0.5°C to 2°C with the thermal properties of the ceramic (+50% on temperature difference between IR and OR). These results show a great impact of the material thermal properties on temperature difference between IR and OR. This is mainly due to a difference of thermal conductivity of steel and ceramic, as shown in Table 4.

As with previous simulations, the bearing average temperature is not changed by the modification of the thermal material properties of the rollers.

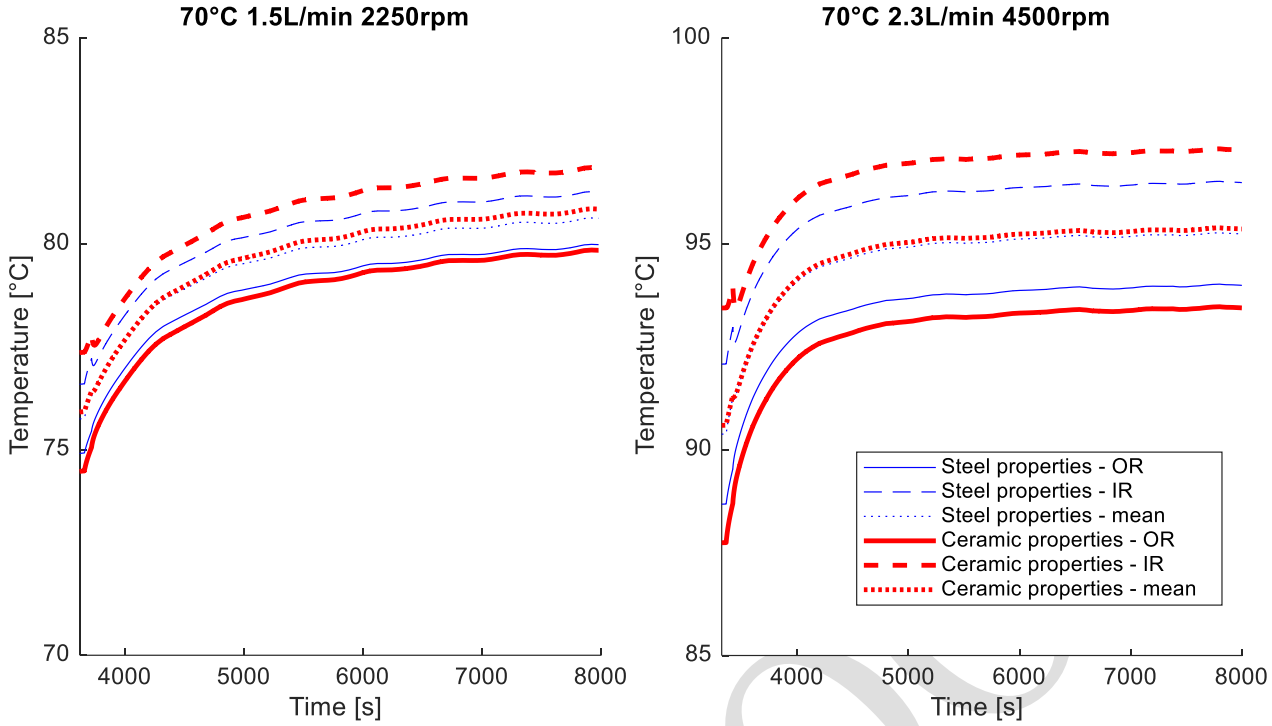

Figure 9 : Impact of material elastic modulus, Poisson's coefficient and thermal conductivity on bearing temperatures

7.3. Impact of mechanical material properties alone

As already mentioned, the mechanical properties of the ceramic rollers result in a calculated contact area reduced by 7% in the studied case (iso-load condition). This modification of the contact area induces an increase of 5% on the temperature difference between IR and OR. Although the impact of mechanical properties is of second order, it should not be neglected.

Another simulation is performed by changing only the mechanical properties of the rolling elements. Thermal properties of the material are kept the same and are the steel roller ones. Moreover, the loading condition of the hybrid bearing is modified: the comparison is conducted at iso-pressure (2.34 GPa). In this case, the calculated contact area is reduced by 16%. The simulation results show that the temperature difference between IR and OR is increased by 10% with the ceramic rollers.

As with previous simulations, the bearing average temperature is not changed by the modification of the mechanical material properties of the rollers.

7.4. Investigation on hybrid bearing power losses

Power loss was proposed as an explanation for the difference between experimental and numerical temperature results in the case of the hybrid bearing.

The following hypothesis is proposed: it is considered that temperature difference between full-steel and hybrid bearings is only due to power losses. Full-steel bearing power losses are the reference for this investigation. Using the thermal network, hybrid bearing power losses are modified until a good temperature correlation between simulation and experiment is observed. As a result, the power losses in steady state regime are obtained and compiled in Table 7.

From this approach, it can be concluded that a 14.8% increase of the average power losses is required to match experimental and simulated average bearing temperatures. This result shows that it is fully possible to model average temperature increase thanks to power losses modification.

7.5. Conclusion on hybrid bearing power losses and thermal exchanges

The simulations conducted thanks to the thermal model showed that both mechanical and thermal properties of the material have an impact on the temperature difference between inner and outer ring. When the material is changed from steel to ceramic, these properties are changed. Thus, both the material thermal properties and the contact surface area in the bearing are modified, resulting in an increase of the temperature difference between the inner and outer ring by up to 3°C with the hybrid TRB. The difference on the thermal conductivity value of ceramic and steel is the main property that drives the thermal exchanges between rollers and races. Still, the mechanical material properties of the ceramic induce a smaller contact surface area that also reduces the thermal exchanges.

The second set of simulations showed that the difference measured on the average bearing temperature should be attributed to a modification of the power losses in the bearing when changing from full-steel to hybrid TRB. Power losses were estimated to be increased by 14.8% on average with the hybrid bearing compared to full-steel bearing. This means also that power losses of the hybrid bearing, initially calculated by using the same friction law as for the full-steel bearing,

are underestimated. So, the friction coefficient could be greater for steel-ceramic contacts than for steel-steel contacts in tapered roller bearings.

An important observation is that the increase of power losses alone does not induce a modification of the temperature difference between IR and OR, while the change of material properties does not influence the bearing average temperature. The two phenomena are independent of each other.

Table 7 : Estimation of the hybrid bearing power losses in steady state regime

Oil temperature (°C)	**40**				**70**			
Oil flow (L/min)	**1.5**		**2.3**		**1.5**		**2.3**	
Rotation speed (rpm)	**2250**	**4500**	**2250**	**4500**	**2250**	**4500**	**2250**	**4500**
Full-steel reference power loss (W)	266	695	255	624	226	593	231	563
Hybrid estimated power loss (W)	293	735	301	702	293	738	290	656
ΔP_{loss} hybrid – full-steel	+27 W (+9.3%)	+41 W (+5.5%)	+46 W (+15.3%)	+78 W (+11.1%)	+67 W (+22.8%)	+145 W (+19.7%)	+59 W (+20.4%)	+94 W (+14.3%)

8. Conclusion

A thermal study was conducted to compare full-steel and hybrid tapered roller bearings and investigate the impact of the use of ceramic rollers on heat generation and bearing temperatures.

Experiments were conducted on a dedicated test rig to measure temperatures of bearings and test rig components. This allowed a first comparison between full-steel and hybrid TRB: in most cases, the hybrid bearing had a higher temperature; the temperature difference between inner and outer ring was always greater for the hybrid bearing.

Numerical investigations were finally conducted to understand the origin of temperature differences observed experimentally between full-steel and hybrid TRB. To this end, a thermal model of the test rig was developed and validated thanks to experimental results obtained on the test rig.

Simulations showed that the greater temperature difference between inner and outer rings measured on the hybrid bearing is mainly due to the thermal properties of the roller material. Indeed, the thermal conductivity of ceramic is lower than the steel one, reducing the thermal exchanges. Although of second order, the mechanical properties of the ceramic induce a smaller contact surface area, also reducing the thermal exchanges.

Another set of numerical investigations showed that the difference measured on the average bearing temperature between full-steel and hybrid bearings can be explained by an increase of the power losses in the case of the hybrid TRB (+14.8% on power losses with the hybrid bearing, compared to full-steel bearing). A possible explanation for this power loss increase is that the friction coefficient could be greater for steel-ceramic contacts than for steel-steel contacts in tapered roller bearings. It is also possible that changing the mass of the rolling elements may impact the dynamic behavior of bearing, impacting skidding sliding, or cage ball contact behavior.

These investigations also showed that the increase of average bearing temperature and the temperature difference between inner and outer ring were independent.

It should be noted that thermal behavior of the studied bearing depends on multiple parameters such as: (i) heat exchanges, mainly from convection with injected oil (in this study, more that 75% of the generated heat is evacuated by the oil); (ii) heat generation in the contact, that represent the main source of power losses, and is dependent on lubrication regime (mixed in this study).

As far as the last item is concerned, a deeper tribological study is required to have a better understanding of the friction of a steel-ceramic contact.

9. Acknowledgement

The authors would like to thank the European Union for its funding. Indeed, this study is part of HEROe bearing project which is funded by CLEANSKY 2 Program (GAP785400).

10. References

1. Wang LRWL, Snidle RW, Gu L. Rolling contact silicon nitride bearing technology: a review of recent research. Wear. 2000; 246(1-2): 159-173.
2. Gloeckner P, Martin M, Flouros M. Comparison of Power Losses and Temperatures between an All-Steel and a Direct Outer Ring--Cooled, Hybrid 133-mm-Bore Ball Bearing at Very High Speeds. Tribology Transactions. 2017; 60(6): 1148-1158.
3. Cento P, Dareing DW. Ceramic materials in hybrid ball bearings. Tribology transactions. 1999; 42(4): 707-714.

4. Paleu V, Olaru DN, Cretu S. Power loss prediction for a hybrid rolling bearing. In Conference Paper, Gheorghe Asachi Technical University of Iasi; 2000.
5. Shoda Y, Ijuin S, Aramaki H, Yui H, Toma K. The performance of a hybrid ceramic ball bearing under high speed conditions with the under-race lubrication method. Tribology Transactions. 1997; 40(4): 676-684.
6. Paleu V, Damian I, Stirbu C. Friction Torque Measurement in Partial Hybrid S-C Angular Contact Ball Bearings. Applied Mechanics and Materials. 2014; 658: 339-344.
7. Aramaki H, Shoda Y, Morishita Y, Sawamoto T. The performance of ball bearings with silicon nitride ceramic balls in high speed spindles for machine tools. ASME Journal of Tribology. 1988; 110: 693-698.
8. Changenet C, Oviedo-Marlot X, Velex P. Power Loss Predictions in Geared Transmissions Using Thermal Networks-Applications to a Six-Speed Manual Gearbox. Journal of Mechanical Design. 2005; 128(3): 618-625.
9. Pouly F, Changenet C, Ville F, Velex P, Damiens B. Power loss predictions in high-speed rolling element bearings using thermal networks. Tribology Transactions. 2010; 53(6): 957-967.
10. Niel D, Changenet C, Ville F, Octrue M. Thermomecanical study of high speed rolling element bearing: A simplified approach. Proceedings of the IMechE, Part J: Journal of Engineering Tribology. 2019; 233(4): 541-552.
11. Neurouth A, Changenet C, Ville F, Arnaudon A. Thermal modeling of a grease lubricated thrust ball bearing. Proceedings of the IMechE, Part J: Journal of Engineering Tribology. 2014; 228(11): 1266-1275.
12. Holman J. Heat transfert. tenth edition ed.: McGraw-Hill; 2010.
13. Durand de Gevigney J, Changenet C, Ville F, Velex P. Thermal modelling of a back-to-back gearbox test machine: Application to the FZG test rig. Proceedings of the IMechE, Part J: Journal of Engineering Tribology. 2012; 226(6): 501-515.
14. Blok H. Les températures de surface dans des conditions de graissage sous extrême pression. In 2nd World Petroleum Congress; 1937.

X : Seoudi, T., Philippon, D., Fillot, N. *et al.* CdSe-Based Quantum Dots as In Situ Pressure and Temperature Non-intrusive Sensors in Elastohydrodynamic Contacts. *Tribol Lett* **68**, 73 (2020). https://doi.org/10.1007/s11249-020-01312-x

Y : Eyring, Henry. “Viscosity, Plasticity, and Diffusion as Examples of Absolute Reaction Rates.” *The Journal of Chemical Physics*, vol. 4, 1936, pp. 283–91, doi:10.1063/1.1749836.

Z : Greenwood, J. A., and J. H. Tripp. “The Contact of Two Nominally Flat Rough Surfaces.” *Proceedings of the Institution of Mechanical Engineers*, vol. 185, no. 14, 1970.